Stability of smectic phases in the Gay–Berne model

Enrique de Miguel
Departamento de Física Aplicada, Facultad de Ciencias Experimentales, Universidad de Huelva, 21071 Huelva, Spain

Elvira Martín del Río
Departamento de Ingeniería Eléctrica y Térmica, Escuela Politécnica Superior de La Rábida, Universidad de Huelva, 21819 Huelva, Spain

Felipe J. Blas
Departamento de Física Aplicada, Facultad de Ciencias Experimentales, Universidad de Huelva, 21071 Huelva, Spain

(Received 10 June 2004; accepted 3 September 2004)

We present a detailed computer simulation study of the phase behavior of the Gay–Berne liquid crystal model with molecular anisotropy parameter $\kappa=4.4$. According to previous investigations: (i) this model exhibits isotropic (I), smectic-A (Sm-A), and smectic-B (Sm-B) phases at low pressures, with an additional nematic (N) phase between the I and Sm-A phases at sufficiently high pressures; (ii) the range of stability of the Sm-A phase turns out to be essentially constant when varying the pressure, whereas other investigations seem to suggest a pressure-dependent Sm-A range; and (iii) the range of stability of the Sm-B phase remains unknown, as its stability with respect to the crystal phase has not been previously considered. The results reported here do show that the Sm-A phase is stable over a limited pressure range, and so it does not extend to arbitrarily low or high pressures. This is in keeping with previous investigations of the effect of molecular elongation on the phase behavior of Gay–Berne models. A detailed study of the melting transition at various pressures shows that the low-temperature crystalline phase melts into an isotropic liquid at very low pressures, and into a nematic liquid at very high pressures. At intermediate pressures, the crystal melts into a Sm-A liquid and no intermediate Sm-B phase is observed. On the basis of this and previous investigations, the reported Sm-B phase for Gay–Berne models appears to be a molecular solid rather than a smectic liquid phase.
[DOI: 10.1063/1.1810472]

I. INTRODUCTION

It is well known that when a crystalline solid is heated at constant pressure, the thermal motion of the molecules increases and the solid expands up to a characteristic temperature beyond which the solid looses its identity and transforms into a liquid. For many simple materials, this melting transition implies the onset of full three-dimensional translational invariance: in the liquid phase, the average density is spatially uniform whereas it is periodic in the solid phase. For complex materials consisting of anisotropic molecules, the presence of orientational degrees of freedom may change drastically this scenario. In addition to the positional order, the solid has (long-range) orientational order, and both types of order are not necessarily lost simultaneously at the melting transition. Instead, the solid may melt into a fluid phase that preserves the orientational order while the translational order is either fully or partially absent. Among the materials that exhibit one or more of these intermediate phases, the most extensively studied are liquid crystals.[1–5] (There are molecular crystals in which a rotational transition precedes the melting transition, giving rise to what is called a *plastic crystal phase*; see, for instance, Chandrasekhar.[1])

The structure of the molecules that form liquid crystals may be quite complex. As a result, it is not straightforward to build models that provide a realistic account of the molecular interactions. Although progress has been made in the field of realistic modeling of liquid crystals,[6,7] the computer implementation of these models is highly demanding, and so their applicability is limited to the study of specific properties under very specific, and necessarily limited, thermodynamic conditions. Alternatively, the use of simpler models allows for a more systematic investigation of the role played by particular features of the interactions on the system properties. Among others, the Gay–Berne (GB) model is one of the most widely used in computer simulation of thermotropic liquid crystals.

In the GB interaction model[8] molecules are considered as rigid units with axial symmetry. Molecule ith is represented by the position vector $\mathbf{r}_i$ of its center of mass and a unit vector $\hat{\mathbf{u}}_i$ along its symmetry axis with respect to an arbitrary (fixed) reference frame. The intermolecular potential energy between two arbitrary molecules i and j is given by

$$U_{ij}^{\mathrm{GB}}(\mathbf{r}_{ij},\hat{\mathbf{u}}_i,\hat{\mathbf{u}}_j)=4\epsilon(\hat{\mathbf{r}}_{ij},\hat{\mathbf{u}}_i,\hat{\mathbf{u}}_j)\left[\left(\frac{\sigma_0}{d(\mathbf{r}_{ij},\hat{\mathbf{u}}_i,\hat{\mathbf{u}}_j)}\right)^{12}-\left(\frac{\sigma_0}{d(\mathbf{r}_{ij},\hat{\mathbf{u}}_i,\hat{\mathbf{u}}_j)}\right)^{6}\right], \quad (1)$$

where $d(\mathbf{r}_{ij},\hat{\mathbf{u}}_i,\hat{\mathbf{u}}_j)=r_{ij}-\sigma(\hat{\mathbf{r}}_{ij},\hat{\mathbf{u}}_i,\hat{\mathbf{u}}_j)+\sigma_0$. Here σ_0 defines the smallest molecular diameter, r_{ij} is the distance between the centers of mass of molecules i and j, and $\hat{\mathbf{r}}_{ij}=\mathbf{r}_{ij}/r_{ij}$ is a unit vector along the intermolecular vector $\mathbf{r}_{ij}=\mathbf{r}_i-\mathbf{r}_j$. The range σ and the strength ϵ of the GB intermolecular potential depend on $\hat{\mathbf{u}}_i$, $\hat{\mathbf{u}}_j$, and $\hat{\mathbf{r}}_{ij}$, as well as on two anisotropy parameters, the ratio of molecular length to breadth, κ, and the ratio of the potential well depths for the side-by-side and end-to-end configuration, κ'. In addition, the anisotropy of the well depth ϵ is also controlled by two other parameters μ and ν. Explicit expressions for σ and ϵ may be found in the original paper by Gay and Berne.[8] In fact, the GB interactions given in Eq. (1) define a family of potential models each characterized by the particular choice of parameters κ, κ', μ, and ν. Note that for the choice $\kappa=\kappa'=1$, the GB potential reduces to the well-known Lennard-Jones potential with $\sigma=\sigma_0$ and $\epsilon=\epsilon_0$ irrespective of the values for μ and ν.

In their seminal work[8] Gay and Berne considered the anisotropy parameters $\kappa=3$, $\kappa'=5$, along with the values $\mu=2$ and $\nu=1$. This parametrization has been widely used in computer simulation studies of the phase behavior.[9–12] In addition, it has been the basis of different theoretical investigations.[13,14] For this choice of parameters, the GB fluid exhibits a weak first-order isotropic-nematic (I-N) transition for temperatures above $T=0.85$ (expressed in the usual reduced units of ϵ_0/k_B, with k_B being Boltzmann's constant). At sufficiently high densities, the nematic fluid freezes into a crystal (Cr) phase. For temperatures below $T=0.85$, nematic ordering is no longer stable and the isotropic fluid directly freezes into the solid phase. This temperature locates the isotropic-nematic-solid triple point, characterized by a pressure $P=2.70$ in conventional reduced units of ϵ_0/σ_0^3. At an even lower temperature ($T\approx 0.47$) there exists a critical point below which vapor-(isotropic) fluid separation takes place over a rather small range of temperatures. Further details may be found in de Miguel and Vega.[12] We recall that *no stable smectic phases* were found for this set of parameters.

In fact, the value $\kappa=3$ for the molecular elongation parameter seems to be close to the (lower) limit of stability of the smectic-A (Sm-A) phase.[15,16] As shown by Brown *et al.*,[16] there is a growth of a stable Sm-A island in the phase diagram at elongations slightly above $\kappa=3$. It was observed that the range of stability of the Sm-A phase extends to both higher and lower temperatures as κ is increased. The phase diagram topology compatible with the simulation results reported by Brown *et al.*[16] is depicted in Fig. 1. Particularly, for elongations $3.0<\kappa<3.6$, the Sm-A phase is bounded both above and below by nematic and solid phases [Fig. 1(a)]. On the other hand, for molecular elongations $3.6\leqslant\kappa\leqslant 4.0$, the Sm-$A$ phase is bounded above by nematic and solid phases and below by isotropic and solid phases [Fig. 1(b)].

Bates and Luckhurst[17] (hereafter, referred to as BL) have reported a constant-pressure Monte Carlo simulation study of the phase behavior of GB fluids with parameters $\kappa=4.4$, $\kappa'=20$, with $\mu=\nu=1$. Varying the temperature along three isobars, these authors identify I, N, Sm-A and smectic-B (Sm-B) phases. In the order of decreasing temperature, they report a phase sequence: (a) $I-N-$Sm-A at pressure $P=3.0$ (no Sm-B phase is reported at this pressure); (b) $I-N-$Sm-$A-$Sm-B at pressure $P=2.0$; and (c) $I-$Sm-$A-$Sm-B at pressure $P=1.0$. All transitions were found to be first order, although the entropy, enthalpy, and density changes at the $N-$Sm-A transition were very small and difficult to measure, and so the possibility of a continuous $N-$Sm-A transition was not ruled out. In keeping with previous simulation results for smaller molecular elongations,[16] the nematic phase is not stable at low pressures. For $\kappa=4.4$, the nematic phase enters the phase diagram above a Sm-$A-N-I$ triple point, which is estimated to occur at $P\approx 1.25$.

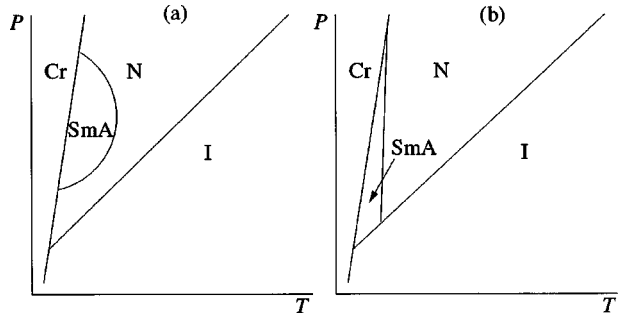

FIG. 1. Topology of the phase diagram (P-T plane) of GB fluids in terms of the molecular elongation κ as deduced from the simulations of Brown *et al.* (Ref. 16) showing isotropic (I), nematic (N), smectic-A (Sm-A), and crystal (Cr) phases. (a) Molecular elongations $3.0<\kappa<3.6$; (b) molecular elongations $3.6\leqslant\kappa\leqslant 4.0$. Although it was reported as smectic-B by Brown *et al.*, the low-temperature phase is denoted here as crystal (see the main text).

The phase diagram emerging from the numerical simulations of BL raises several questions, which are as follows:

(1) The slopes of the Sm-$B-$Sm-A and Sm-$A-N$ phase boundaries are found to be similar, and so the Sm-A range seems to be fairly constant. It would be of interest to know whether for this elongation the Sm-A phase remains unbounded at higher and lower pressures, thus not following the general trend seen earlier by Brown *et al.*[16] [see Fig. 1(b)].

(2) The low-temperature phase for the $\kappa=4.4$ GB fluid is identified as a hexatic (Sm-B) phase (that is, a smectic liquid with short-range in-layer positional order and long-range bond orientational order). As no crystalline phase is reported for this molecular elongation, it would be of interest to explore whether the Sm-$A-$Sm-B transition is followed by a Sm-$B-$Cr transition at lower temperatures.

According to previous simulation investigations, the anisotropic interactions in GB models promote the formation of a layered structure at low temperature (at fixed pressure) or at high density (at fixed temperature) with nearly hexagonal distribution of the molecular centers of mass within the layers. Although typically reported as Sm-B, whether this structure is smecticlike (Sm-B) or crystalline has been always recognized as a subtle problem. As noted by Allen *et al.*[15] for GB models with $3<\kappa\leqslant 4$, no transition to a solid phase could be identified on cooling the Sm-B; indeed, the reported Sm-B phase was found to exhibit well-defined correlations characteristic of solidlike packing. Further evidence of the

(possible) crystalline nature of the Sm-B phase was given by Brown *et al.*[16] On the basis of these results, it seems that the Sm-B phases reported by Allen *et al.*[15] and Brown *et al.*[16] for GB molecular systems with $3<\kappa\leqslant 4$ have in fact a crystalline structure and that it might be more appropriate to refer to them as solids rather than Sm-B phases. We recall that in a more recent investigation of the $\kappa=3$ GB model,[12] the previously designated Sm-B phase seems to be a crystal phase and not a smectic liquid crystal. For the $\kappa=4.4$ GB fluid BL also report no solid but Sm-B phase at low temperatures.[17] In a subsequent paper Bates and Luckhurst[18] report a simulation investigation of the x-ray scattering pattern formed by the $\kappa=4.4$ GB fluid. The results indicate that there are correlations in bond orientational order between the layers of the low-temperature phase. This phase was characterized as a Sm-B phase, although its crystalline nature was not ruled out. Therefore, it remains to be checked whether or not for sufficiently elongated molecules, the GB interactions stabilize a Sm-B phase before full crystallization.

The simulation work reported here concentrates on the phase behavior of the GB fluid with $\kappa=4.4$ using the same set of anisotropy parameters as that used previously by BL.[17] We first compare our simulation results with those reported by BL along two isobars in the (arbitrarily termed) intermediate pressure region where the Sm-A phase has been reported. We then proceed to investigate whether Sm-A ordering shows up at lower and higher pressures. The whole phase sequence at each pressure is studied and the (approximate) transition temperatures are obtained. The possible occurrence of a Cr–Sm-B transition at low temperatures is also investigated. All these results are summarized in a phase diagram showing the regions of stability of all phases found for the $\kappa=4.4$ GB fluid.

Details of the simulation techniques are given in Sec. II, which also includes details on the calculation of the order parameters and distribution functions used to probe the nature of the various phases. The simulation results concerning the phase behavior are presented in Sec. III, where they are compared (when appropriate) with the results reported by BL. The analysis of the order parameters and structural functions is presented in Sec. IV. Finally, we summarize our main findings and conclusions in Sec. V.

II. SIMULATION DETAILS

A. General features

We have used constant-pressure Monte Carlo simulations to investigate the behavior of GB systems with molecular elongation $\kappa=4.4$. The values of the other anisotropy parameters that define the intermolecular interactions are set equal to those used by BL,[17] namely, $\kappa'=20$ and $\mu=\nu=1$. In order to be able to compare with previous results, the intermolecular interactions were truncated at $r_c=5.5\sigma_0$ and no long-range corrections were applied. Standard periodic boundary conditions were used.

We have obtained the equation of state for different values of the pressure. In all cases, simulations were started at low temperature from a crystalline solid structure consisting on a set of layers parallel to the xy plane with in-layer hexagonal arrangement of the molecular centers of mass. The layers are stacked following an ABC structure analogous to that of the fcc lattice and stretched along z. All molecules were initially oriented perpendicular to the layers, thus pointing along z. Six layers were considered, each layer consisting of 15×18 molecules. This arrangement yields a total of $N=1620$ molecules.

The simulations were organized in cycles, each cycle consisting of N attempts to displace or rotate the molecules and two or three trial volume fluctuations, as explained below. At each input temperature, the system was typically equilibrated for 75 000 cycles; thermodynamic properties, order parameters, and appropriate distribution functions were averaged over 25 000 additional cycles. Near a transition, however, runs at least twice as long were performed in order to ensure proper equilibration.

Depending on the nature of the simulated state point, we considered three different algorithms to keep the pressure constant. In all cases, the box was kept orthorhombic during the simulation and therefore, the box sides L_x, L_y, L_z were constrained to be mutually orthogonal throughout the simulation. For phases with no translational order (isotropic and nematic), volume changes were made isotropically and therefore the box lengths kept the same (input) ratio. In such cases, two trial changes were attempted per cycle. This scheme is certainly not appropriate for phases with translational order (smectic or solid) because the system has to fit an ordered structure into a box of fixed shape and this may result in unbalanced strain on the system. For the smectic phase, two independent types of volume changes were considered per cycle: one in which the box length L_z is attempted to vary, and the other one in which the transverse section of the simulation box is attempted to vary while keeping the box-length ratio L_x/L_y constant. The latter implies trial (isotropic) changes of the area of the smectic layers. For the low-temperature solid phase, volume fluctuations were performed by allowing all three box lengths to vary independently. In such cases, three trial changes were performed per cycle. When a volume change implied two (for the smectic phase) or three (for the solid phase) independent changes in box lengths, they were performed sequentially. The maximum translational/rotational displacements and box-length fluctuations were adjusted in each case so as to obtain an average acceptance of about 30%–35% and 25%, respectively.

The exact location of the various transitions is a problem far from being trivial. In particular, first-order transitions commonly exhibit hysteresis and so the phase transformation proceeds irreversibly beyond the coexistence point. A rigorous location of the various transition temperatures would require the computation of the free energy of all phases.[19] This is however a fairly demanding task, particularly when phases with translational order (such as the solid or the smectic) are involved,[12,19,20] and has not been attempted here. Alternatively, whenever a transition takes place, we have determined the temperature limits of stability of each phase by slowly heating and cooling the system through the transition. The actual transition temperature should be bracketed by these temperature values. If upon heating the system jumps from

phase A to phase B at temperatures T_A and T_B ($T_B > T_A$), respectively, the limit of stability of phase A, T_{AB}, is simply estimated as $T_{AB}=(T_B+T_A)/2$, with an associated error of $(T_B-T_A)/2$. The limit of stability of phase B upon cooling, T_{BA}, is estimated in a similar way. According to our comments above, one should expect $T_{AB} > T_{BA}$ if the (first-order) A-B transition exhibits hysteresis.

In addition, estimates of the values of any property Λ (either thermodynamic average or order parameter) at each side of, say, the A-B transition are obtained as

$$\Lambda_A \equiv \Lambda(T_{AB}^-) = \lim_{T \to T_{AB}^-} \Lambda(T), \tag{2}$$

and similarly

$$\Lambda_B \equiv \Lambda(T_{AB}^+) = \lim_{T \to T_{AB}^+} \Lambda(T). \tag{3}$$

In practice these limiting values were obtained by using a second-order polynomial extrapolation scheme. Typically, a set of four values of property Λ (those closest to the transition temperature) were considered at each side of the transition.

All quantities given below are expressed in conventional reduced units, with σ_0 and ϵ_0 being the units of length and energy, respectively. Thus, the temperature is given in units of ϵ_0/k_B, the pressure is in units of ϵ_0/σ_0^3, and the number density is in units of σ_0^{-3}. Occasionally, the density is expressed as ρ/ρ_{cp}, where $\rho_{\mathrm{cp}}=\sqrt{2}/\kappa$ represents the density that an equivalent system of hard ellipsoids of elongation κ would have at regular close packing. For the present choice of molecular elongation ($\kappa=4.4$), $\rho_{\mathrm{cp}}=0.321\,11$.

B. Structural properties and order parameters

The structure of the different phases was probed by calculating the (orientationally averaged) pair distribution function $g(r)$, as well as the pair distributions $g_\parallel(r_\parallel)$ and $g_\perp(r_\perp)$, which provide information on the distribution of molecules separated by a distance $r_\parallel$ (pair separation parallel to the director of the phase) and $r_\perp$ (pair separation perpendicular to the director), respectively. In the absence of positional correlations (isotropic or nematic phases) $g(r)$ tends to unity and $g_\parallel(r_\parallel)$ is uniform. Smectic layering generates a one-dimensional density wave along the director (which for orthogonal smectics coincides with the layer normal) and so oscillations appear in $g_\parallel(r_\parallel)$. Finally, the distribution $g_\perp(r_\perp)$ probes the in-plane positional correlations within the layers, discriminating between smectic and solid phases. To analyze positional correlations between molecules located in either the same or adjacent layers, we calculated a family of functions $g_{mn}(r_\perp)$, where m and n are integers labeling the layers. $g_{11}(r_\perp)$, for example, is a distribution function averaged over pairs of molecules in the first layer; $g_{12}(r_\perp)$ is defined for pairs in which one molecule is in the first layer and the other one in the second layer.

To facilitate the identification of the different phases, we have calculated a number of order parameters. The orientational order parameter S was calculated in the simulations as the average of the largest eigenvalue of the ordering $Q_{\alpha\beta}$ tensor,[21] defined in terms of the components of the unit vectors along the principal axis of the molecules,

$$Q_{\alpha\beta} = \frac{1}{N}\sum_{i=1}^{N} \frac{1}{2}(3u_{i\alpha}u_{i\beta} - \delta_{\alpha\beta}). \tag{4}$$

S is a measure of the degree of orientational order and may take on values between 0 (fully orientationally disordered fluid) and 1 (perfectly oriented system). The director of the phase is associated to the corresponding eigenvector.

We have also calculated the translational order parameter τ defined from

$$\tau(q) = |\langle \exp(iqr_\parallel)\rangle|. \tag{5}$$

In Eq. (5), the wave vector q is defined as $q=2\pi/d$, with d being related to the (as yet unknown) layer spacing. Note that the definition given in Eq. (5) is closely related to the longitudinal part (along the director) of the static structure factor. In practice, we calculated $\tau(q)$ for a grid of values of q and determined the value q^* associated to the first maximum in $\tau(q)$. The layer spacing d^* follows from $d^*=2\pi/q^*$ and the corresponding value $\tau \equiv \tau(q^*)$ is identified with the translational order parameter. From its definition, τ is a measure of the degree of positional order along the director. Thus, layering in the system will be manifested by nonzero values for the translational order parameter.

Translational in-plane order was monitored by calculating the local bond orientational order.[22] For a particle at position $\mathbf{r}_i$, this is defined as

$$\psi_6(\mathbf{r}_i) = \frac{\sum_j w(R_{ij}) \exp(i6\theta_{ij})}{\sum_j w(R_{ij})}, \tag{6}$$

where the summation is extended over the j nearest neighbors of particle i, and θ_{ij} is the angle between the vector $\mathbf{R}_{ij}$ (projection of the intermolecular vector $\mathbf{r}_{ij}$ onto the layer plane) and a fixed (arbitrary) axis. The weighting function $w(R_{ij})$ appearing in Eq. (6) provides a criterium for selecting the nearest neighbors of each particle.[22] Following Bates and Luckhurst,[17] this function was defined as unity for $R_{ij} < 1.4$, zero for $R_{ij} > 1.8$ and through a linear interpolation in between 1.4 and 1.8. As claimed by BL,[17] the behavior of the local bond orientational order was essentially insensitive to the particular choice of weighting function. From Eq. (6) one may calculate the (average) bond orientational order in each layer as

$$\psi_6^m = \mathrm{Re}\left\{ \frac{1}{N_m} \sum_i \psi_6(\mathbf{r}_i), \right\}, \tag{7}$$

where N_m is the number of molecules in layer m and the sum is restricted to those molecules belonging to layer m. A bulk bond orientational order parameter ψ_6 was calculated by averaging $\psi_6(\mathbf{r}_i)$ over the whole system as

$$\psi_6 = \mathrm{Re}\left\{ \frac{1}{N} \sum_i \psi_6(\mathbf{r}_i) \right\}. \tag{8}$$

Finally we have also computed the in-layer bond orientational order correlation functions

$$g_6^m(r_\perp) = \langle \psi_6(\mathbf{r}_i)\psi_6^*(\mathbf{r}_j)\rangle \tag{9}$$

for molecules belonging to the same layer m. For a crystal (or a Sm-B) phase, with hexagonal in-layer packing, these

functions should be long range and decay to a nonzero value at long distances. For a Sm-*A* phase, on the other hand, they should be short ranged and decay to zero.

III. PHASE BEHAVIOR

Here we present our constant-pressure MC simulation results. We first discuss in some detail the phase behavior observed at intermediate pressures ($P=2.0$ and $P=1.0$) from the analysis of the equation of state and order parameters; then we present the results obtained both at lower ($P=0.4$ and $P=0.2$) and higher ($P=3.0$ and $P=15.0$) pressures.

A. Intermediate pressures ($P=2.0$ and $P=1.0$)

At $P=2.0$ the simulations were started from a defect-free crystal configuration consisting on six molecular layers with in-layer hexagonal packing. This initial configuration was well equilibrated at a reduced temperature $T=0.80$. The final (equilibrated) configuration corresponded to a solid structure with a number density $\rho=0.240\,82(9)$, which corresponds to $\rho/\rho_{cp}=0.75$. The orientational order parameter was $S=0.9875(2)$, the translational order parameter $\tau=0.950(2)$, and the bulk bond orientational order parameter $\psi_6=0.926(1)$. The spacing between adjacent crystal layers was found to be $d^*=3.78$. The system was subsequently heated in small temperature steps. We show in Fig. 2 the variation with temperature of the average number density at $P=2.0$ as well as the values of the different order parameters along the isobar. According to the figure, the system undergoes a number of transitions on heating. The crystal phase experiences a first-order transition at $T=1.33(1)$ with a relative density change of 5.3%. As shown in Fig. 2, at $T=1.34$ (high-temperature side of the transition) there exists significant translational order along z [$\tau=0.696(20)$, the layer spacing being $d^*=3.92$] and a substantial degree of orientational order [$S=0.909(2)$]; furthermore, the value of ψ_6 drops to zero at this temperature [see Fig. 2(b)]. It follows that the crystal phase melts into a Sm-*A* phase. This was further corroborated by the behavior of the distribution functions: the layering in the system shows up as oscillations in $g_{\parallel}(r_{\parallel})$ with a periodicity equal to the calculated value of d^*, and the in-layer distribution functions $g_{nn}(r_{\perp})$ are liquidlike (no positional order of the molecular centers of mass within the layers). In the low-temperature side of the transition the functions $g_{nn}(r_{\perp})$ exhibit considerable structure and are definitely not liquidlike. No intermediate Sm-*B* phase was observed between the Cr and the Sm-*A* phases. This will be discussed in more detail in Sec. IV.

Upon increasing the temperature, the Sm-*A* undergoes a transition to a nematic phase at $T=1.465(5)$. This is confirmed by the values of the translational order parameter [$\tau=0.37(7)$ at $T=1.46$ and $\tau=0.09(3)$ at $T=1.47$]. The relative density change at the transition is rather small (about 0.9%). On increasing the temperature, the nematic phase melts into an isotropic fluid at higher temperature $T=1.690(5)$ via a weak first-order transition, the observed relative density change at the transition being of about 2.3%.

A similar phase sequence is observed by BL *after cooling the system from the isotropic phase* at $P=2.0$, although

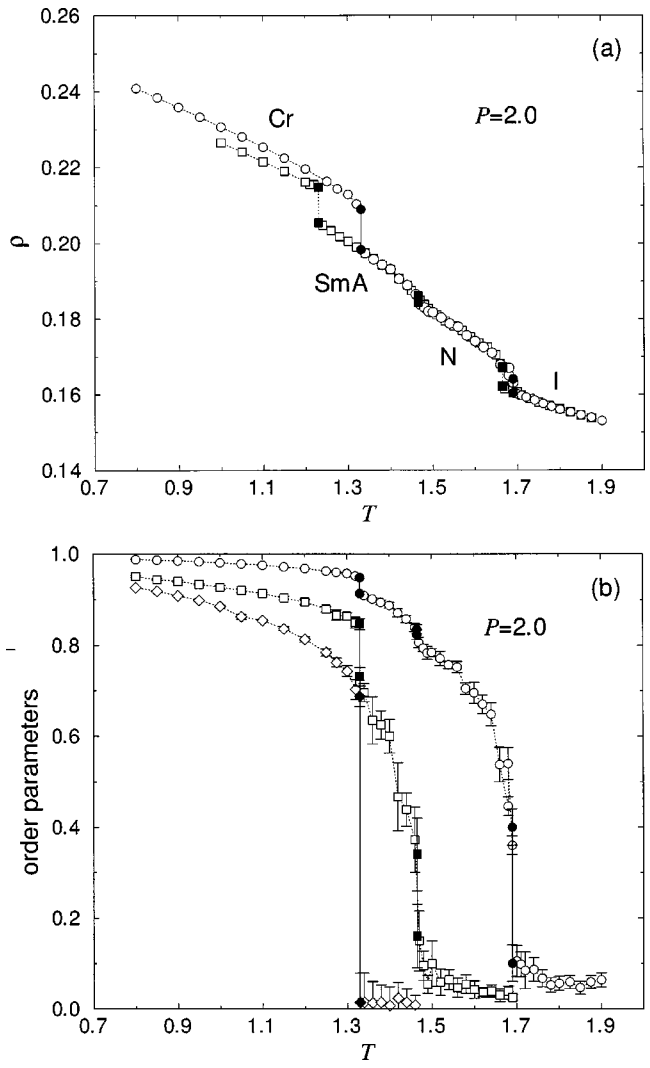

FIG. 2. Simulation results for the $\kappa=4.4$ GB model along the isobar $P=2.0$. (a) Variation with temperature T of the average number density ρ. Circles, increasing temperature; squares, decreasing temperature. (b) Variation with temperature of the order parameters along the heating series. Circles, orientational order parameter S; squares, translational order parameter τ; diamonds, bulk bond orientational order parameter ψ_6. Filled symbols correspond to approximate values at the various transitions.

the low-temperature phase was identified as a Sm-*B* phase. The (approximate) transition temperatures reported by BL for the sequence Sm-*B*–Sm-*A*–*N*–*I* are 1.225(25), 1.475(25), and 1.675(25), respectively.[17] Both sets of temperatures are in agreement with the notable exception of the temperature corresponding to the Sm-*B*–Sm-*A* (or Cr–Sm-*A*) transition. Although this difference may be simply understood in terms of hysteresis at the transition, one should bear in mind that BL explicitly states that no hysteresis was found across this transition. We decided to investigate this point further.

In order to check for possible hysteresis effects, an (independent) isotropic fluid configuration was generated and well equilibrated at high temperature $T=1.90$ well beyond the *I*-*N* transition. This configuration was slowly cooled in small temperature steps. The transition to the nematic phase was observed to take place at a slightly lower temperature $T=1.665(5)$ when compared to the value obtained on heat-

ing. As expected, hysteresis effects, albeit small, are present at the I-N transition. As the temperature was further lowered, the system developed a layered Sm-A structure at $T=1.47$. No density change was found at the $N-$Sm-A transition and hysteresis effects, if present, were negligible. Within the accuracy of the simulation results, it appears that the N transforms continuously into the Sm-A phase. The director of the Sm-A phase pointed closely (but not exactly) along the z direction. In order to facilitate the calculation of the distribution functions, the director of the phase was reoriented along the z axis by applying an aligning external field at $T=1.47$. After running for 1000 cycles, the director was effectively pointing along z. The external field was then switched off and the system was allowed to equilibrate for a further period of 75 000 cycles. The thermodynamic properties were found to be identical (within statistical uncertainties) to those obtained before reorienting the director. Along the rest of the cooling series, the orientation of the director did not change. Finally, the Sm-A phase exhibited a further transition at lower temperature accompanied by an increase in the average number density (see Fig. 2) at $T=1.22$. At this temperature there were six layers in the simulation box. The value of the bond orientational order parameter in the two central layers of the simulation box was found to be about 0.80, and between 0.32 and 0.44 in the other (four) layers. These values were found to remain essentially unchanged after running over a further period of 400 000 cycles. This low-temperature phase seems to be an imperfect solid. On cooling from the Sm-A phase, the system seems to quench defects in the crystalline structure and this results in a larger available volume per particle (lower average density) in comparison to the values expected in a crystal structure with no defects. This would explain why the average densities obtained on cooling are slightly, but systematically, lower than those obtained in the heating series in the low-temperature region (see Fig. 2). In principle, one might anticipate that the growth of a perfect, defect-free crystalline solid on cooling from a fluid phase must be a process difficult to achieve in simulation even for the simpler model fluids. Besides, this process is expected to strongly depend, among other factors, on the particular history of the cooling process. In any event, this temperature ($T=1.22$) provides an indication of the lower limit of stability of the Sm-A phase. This temperature should be compared with the above-mentioned value $T=1.33(1)$ for the upper limit of stability of the crystal phase.

Summarizing, the phase sequence observed at $P=2.0$ is

$$\mathrm{Cr} \underset{1.23(1)}{\overset{1.33(1)}{\rightleftarrows}} \text{Sm-}A \underset{1.475(5)}{\overset{1.465(5)}{\rightleftarrows}} N \underset{1.665(5)}{\overset{1.690(5)}{\rightleftarrows}} I,$$

where the top (bottom) values are the approximate transition temperatures for the heating (cooling) series. The corresponding values obtained by BL along this isobar are in full agreement with our findings *for the cooling series*, although the low-temperature phase is identified there as a Sm-B phase.

A similar procedure was followed for the simulations at lower pressures. The resulting average number density and order parameters along $P=1.0$ in terms of temperature are presented in Fig. 3. The observed phase sequence along the heating and cooling series along this pressure is

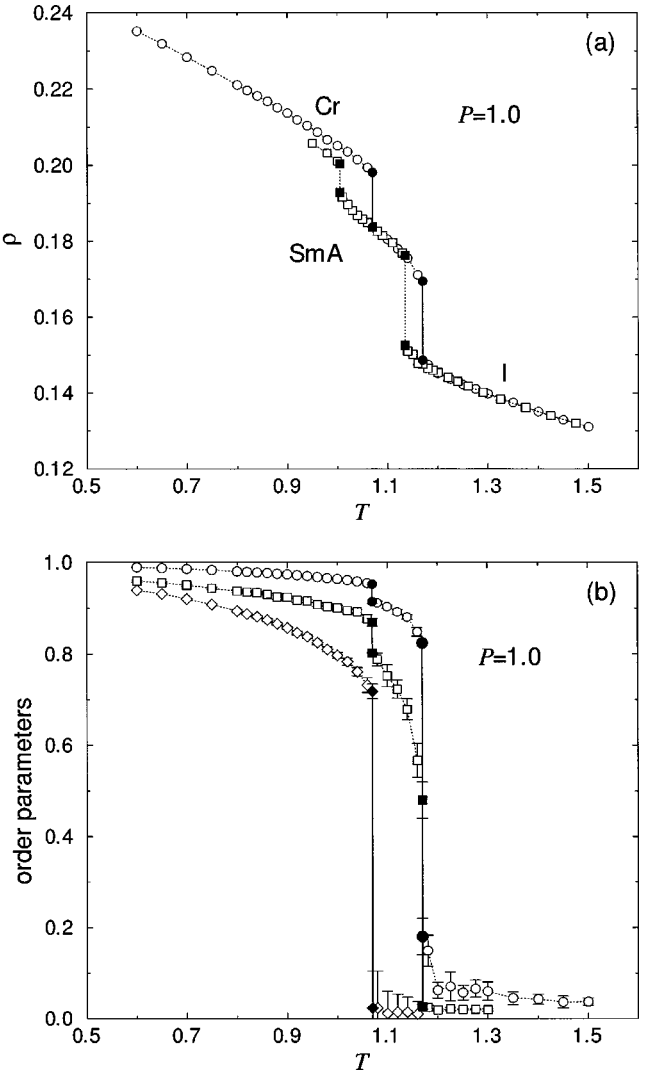

FIG. 3. Simulation results for the $\kappa=4.4$ GB model along the isobar $P=1.0$. (a) Variation with temperature T of the average number density ρ. Circles, increasing temperature; squares, decreasing temperature. (b) Variation with temperature of the order parameters along the heating series. Circles, orientational order parameter S; squares, translational order parameter τ; diamonds, bulk bond orientational order parameter ψ_6. Filled symbols correspond to approximate values at the various transitions.

$$\mathrm{Cr} \underset{1.005(5)}{\overset{1.07(1)}{\rightleftarrows}} \text{Sm-}A \underset{1.135(5)}{\overset{1.17(1)}{\rightleftarrows}} I,$$

where the numbers indicate the (approximate) transition temperatures. In agreement with previous results,[17] no nematic phase is observed at this pressure. This points to the existence of a Sm-$A-N-I$ triple point at some intermediate pressure value between 1.0 and 2.0. The triple point temperature must lie somewhere between 1.00 and 1.45. We do find hysteresis at both transitions, the effect being particularly noticeable at the Cr–Sm-A transition. Once smectic-A layering showed up in the cooling series ($T=1.13$), the director was reoriented along z applying an external orienting field. As before, no effect on the thermodynamic properties were

observed after switching the field off and equilibrating the system; therefore, the external field did have no side effects on the structure of the Sm-A other than reorienting the director. The transition temperatures reported by Bates and Luckhurst[17] for the sequence Sm-B–Sm-A–I are 0.95(5) and 1.15(5) (no hysteresis is reported there), which are in agreement with the values found here for the transition temperatures along the cooling series. As for $P=2.0$, the low-temperature phase seems to be crystalline and no Cr–Sm-B transition is observed.

B. Low pressures ($P=0.4$ and $P=0.2$)

The above results seem to indicate that the range of temperatures over which the system exhibits Sm-A phase gets smaller as the pressure is decreased. This is further illustrated in Fig. 4, where the simulation results for the average number density in terms of temperature at $P=0.4$ are presented along with the corresponding values of the order parameters. On heating from low temperature, the crystal is observed to melt into a Sm-A liquid at $T=0.88$, although the layering gets rapidly destabilized at a slightly higher temperature $T=0.91$: at this temperature, the Sm-A phase melts into an isotropic liquid. This temperature range is rather narrow and it may well occur that the Sm-A phase is metastable at this pressure. We note that no Sm-A phase was found when cooling an isotropic liquid at $P=0.4$, the fluid transforming directly into an imperfect crystal structure. From these simulations, the approximate transition temperatures along $P=0.4$ are

$$\mathrm{Cr} \underset{0.815(5)}{\overset{0.87(1)}{\rightarrow}} \text{Sm-}A \overset{0.905(5)}{\rightarrow} I.$$

At even lower pressure, the absence of Sm-A ordering is clearly manifested. The simulations carried out at $P=0.2$ indicated that the solid phase melts directly into an isotropic fluid with no intermediate Sm-A phase. This is further confirmed after cooling an isotropic liquid at this pressure: the isotropic liquid transforms directly into an imperfect crystalline structure. The corresponding results are shown in Fig. 4. The approximate transition temperatures are

$$\mathrm{Cr} \underset{0.71(5)}{\overset{0.79(1)}{\rightleftarrows}} I.$$

Again, the solid-to-fluid transition exhibits hysteresis. The results of the simulations performed in the low-pressure region indicate that the range of stability of the Sm-A does not extend to arbitrarily low pressures (or temperatures) but is definitely bounded from below by a Cr–Sm-A–I triple point. This scenario is consistent with the predictions emerging from previous simulation results of the GB fluid.[16]

C. High-pressure region

It remains to check the behavior of the $\kappa=4.4$ GB fluid at higher pressures. We recall that Sm-A behavior was observed at $P=3.0$ by BL (Ref. 17) (in addition to nematic and isotropic phases at sufficiently high temperatures). Although it is claimed there that a Sm-B phase should follow the Sm-A phase on cooling, this transition was not investigated; hence, the temperature range over which the Sm-A is stable at this pressure is unknown.

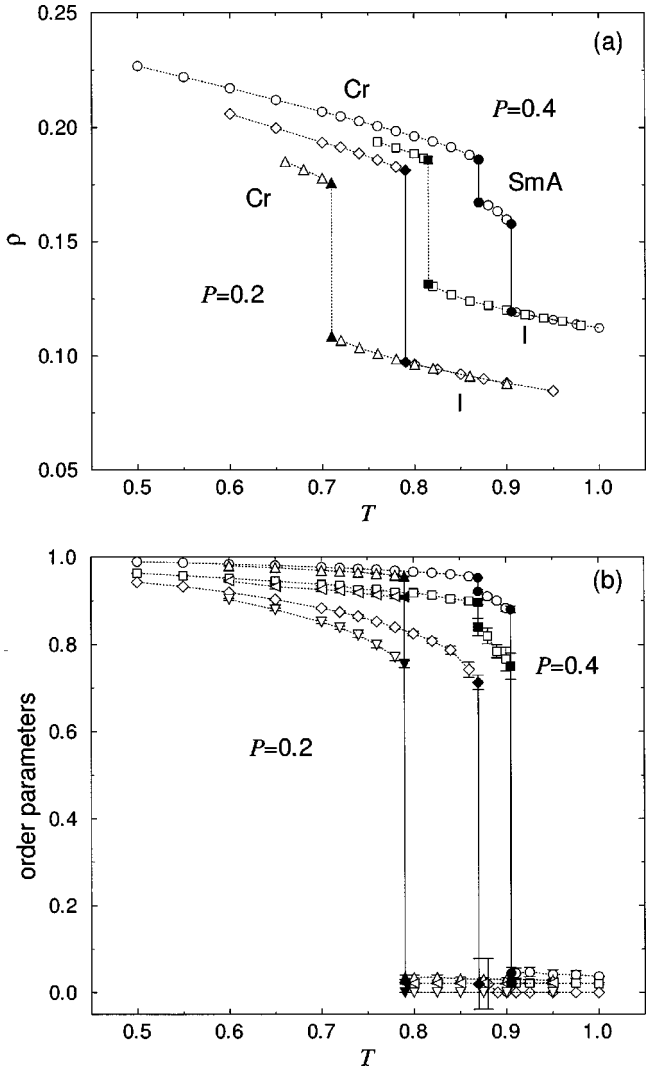

FIG. 4. Simulation results for the $\kappa=4.4$ GB model along the isobars $P=0.4$ and 0.2. (a) Variation with temperature T of the average number density ρ. Circles and squares, increasing and decreasing temperature, respectively, for $P=0.4$; diamonds and triangles, increasing and decreasing temperature, respectively, for $P=0.2$. (b) Variation with temperature of the order parameters along the heating series. Circles and up-triangles, orientational order parameter for $P=0.4$ and $P=0.2$, respectively; squares and left-pointing triangles, translational order parameter for $P=0.4$ and $P=0.2$, respectively; diamonds and down-triangles, bulk bond orientational order parameter for $P=0.4$ and $P=0.2$, respectively. Filled symbols correspond to approximate values at the various transitions.

The phase sequence, including the approximate transition temperatures, obtained here along $P=3.0$ is

$$\mathrm{Cr} \underset{1.41(1)}{\overset{1.54(1)}{\rightleftarrows}} \text{Sm-}A \underset{1.66(1)}{\overset{1.6625(25)}{\rightleftarrows}} N \underset{2.17(1)}{\overset{2.18(1)}{\rightleftarrows}} I.$$

For comparison, the (approximate) transition temperatures reported by Bates and Luckhurst[17] are 1.70(10) and 2.175(25) for the Sm-A–N and N-I transitions, respectively, these values being fully consistent with our approximate values. Unfortunately, our results along $P=3.0$ did not allow us to draw any conclusion about the behavior of the Sm-A

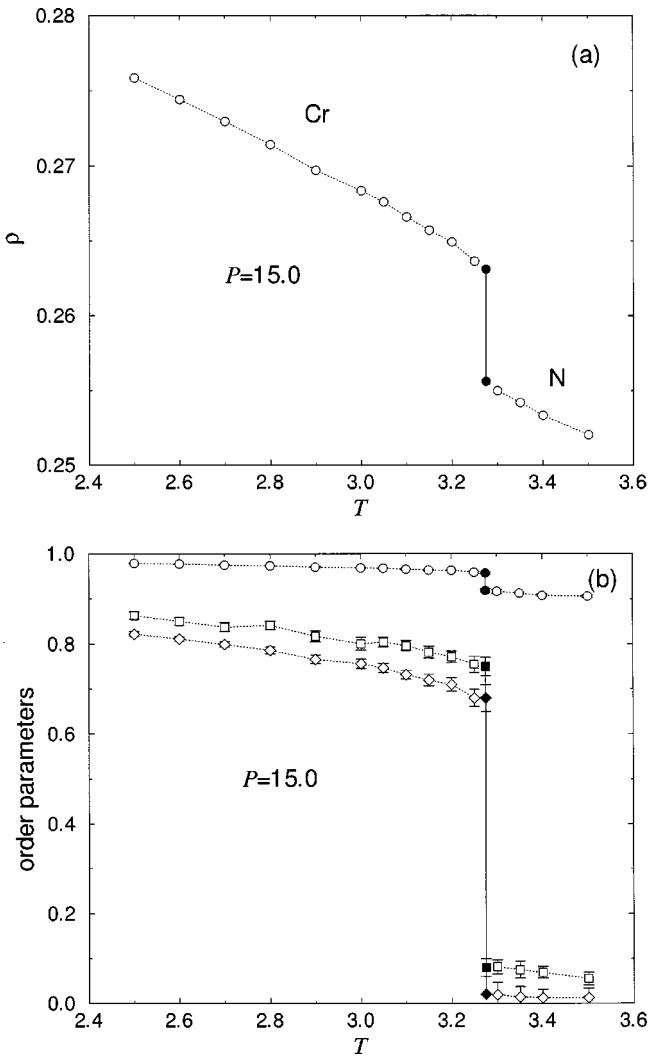

FIG. 5. Simulation results for the $\kappa=4.4$ GB model along the isobar $P=15.0$. (a) Variation with temperature T of the average number density ρ along the heating series. (b) Variation with temperature of the order parameters along the heating series. Circles, orientational order parameter S; squares, translational order parameter τ; diamonds, bulk bond orientational order parameter ψ_6. Filled symbols correspond to approximate values at the Cr-N transition.

range with increasing pressure: this range was found to be almost insensitive to an increase in pressure from $P=2.0$ to a value $P=3.0$.

At substantially higher pressures, however, there were clear indications that the Sm-A phase was absent. This is shown in Fig. 5, where simulation results obtained on heating a crystalline solid at $P=15.0$ are presented. At temperature $T=3.275(25)$ the solid phase melts into a highly dense liquid ($\rho/\rho_{cp}\approx 0.80$). The fluid phase is orientationally ordered ($S\approx 0.920$) but translational order is fully absent: both τ and ψ_6 drop to zero at the transition. According to this, the crystal phase melts into a nematic, the transition not being mediated by any smectic phase.

The pressure-temperature projection of the phase diagram emerging from the present work is presented in Fig. 6. The low-temperature phase corresponds to a crystalline solid. At low pressures, no liquid crystal phases are observed and the crystal phase directly melts into an isotropic liquid.

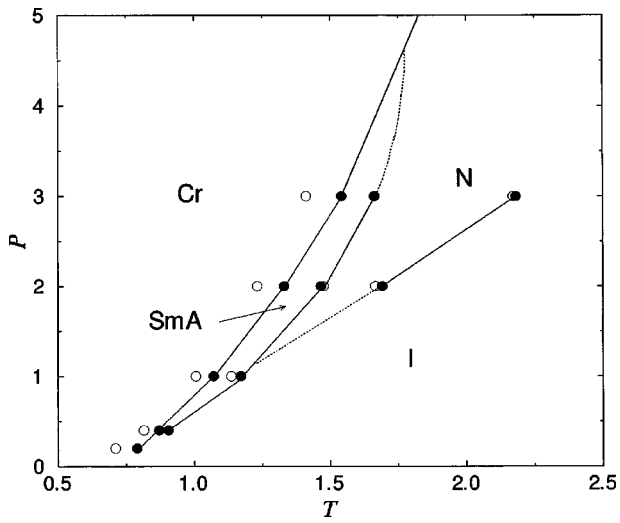

FIG. 6. Approximate phase diagram for the $\kappa=4.4$ GB model in the P-T plane showing isotropic (I), nematic (N), smectic-A (Sm-A), and crystal (Cr) phases. Filled circles correspond to the (approximate) transition temperatures obtained on heating; open circles correspond to those obtained on cooling. Discontinuous lines are extrapolations of the simulation results.

Mesomorphism is induced in the system with increasing applied pressure. Above a pressure value $P\approx 0.4$, the crystal melts into an intermediate Sm-A liquid, and the Sm-A phase melts at higher temperatures into an isotropic liquid. All these transitions involve both a density and enthalpy change and are therefore first order. At higher applied pressure, nematic ordering is developed in between the Sm-A and I phases. This occurs for pressures above $P\approx 1.25$. Small density and enthalpy changes are observed at the Sm-A–N transition and so the transition is either very weakly first order or even continuous. The N-I transition occurring at higher temperatures is definitely (weakly) first order. The nematic range increases with pressure. On the other hand, the Sm-A is found to be stable over a small range of temperatures. According to our results, the Sm-A phase does not extend to arbitrarily high pressure, and so the Sm-A–N line should intersect the Cr–Sm-A line at a well-defined value of the pressure. This value has not been calculated but we give an estimate in the following section. Note that the continuation of the N–Sm-A transition line at high pressures in Fig. 6 (drawn there as a dotted line) is merely a guide to the eye. We emphasize that the lines in Fig. 6 do not represent coexistence lines, as no free-energy calculation has been performed whatsoever. As most transitions do show hysteresis (particularly those involving the crystal phase) the limits of stability of each phase upon heating and cooling do not coincide: the actual transition temperature (in a thermodynamic sense) should be bracketed by these limits. The topology of the phase diagram of the $\kappa=4.4$ GB model is therefore in agreement with the predictions of Brown *et al.*[16] (see Fig. 1).

IV. ORDER PARAMETERS AND STRUCTURAL PROPERTIES

We now turn to examine the behavior of the various order parameters defined in Sec. II B in the range of pressures considered in this work. The variation with temperature

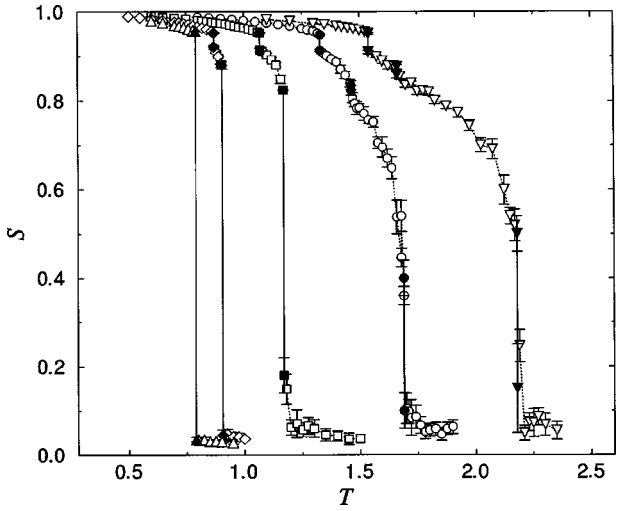

FIG. 7. Variation with temperature T of the orientational order parameter S along the isobars $P=3.0$ (down-triangles), $P=2.0$ (circles), $P=1.0$ (squares), $P=0.4$ (diamonds), and $P=0.2$ (up-triangles). Filled symbols correspond to approximate values at the various transitions.

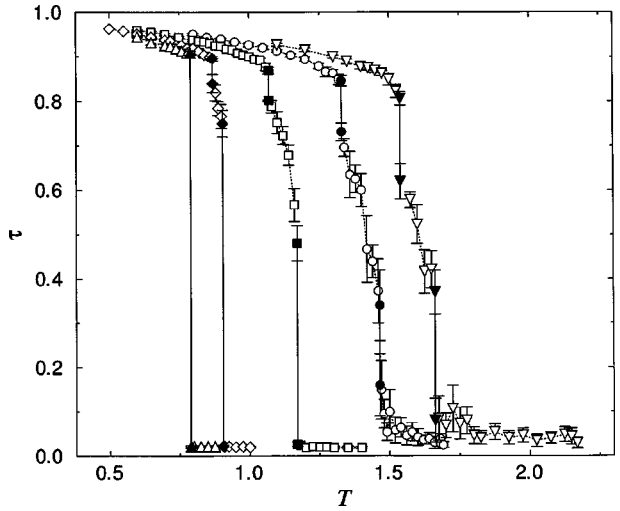

FIG. 8. Variation with temperature T of the translational order parameter τ along the isobars $P=3.0$ (down-triangles), $P=2.0$ (circles), $P=1.0$ (squares), $P=0.4$ (diamonds), and $P=0.2$ (up-triangles). Filled symbols correspond to approximate values at the various transitions.

of the orientational order parameter S is presented in Fig. 7. In the crystal phase, this order parameter is close to 1 and decreases smoothly as the temperature is increased. At its limit of stability, the solid is characterized by values of S of about 0.950, the actual value being rather insensitive to pressure. As can be observed in Fig. 7, the Cr–Sm-A transition is always accompanied by a small but measurable jump in the orientational order parameter (of about 0.04 on heating and 0.03 on cooling) at all pressures. This increase in orientational disorder seems to be associated to the increase in the available volume per particle at the melting transition. Along the Sm-A phase, the orientational order decreases with increasing temperature. At the Sm-A side of the transition to the nematic phase, we found $S=0.876(5)$ (at $P=3.0$) and $S=0.835(10)$ (at $P=2.0$). Again, there appears to be a small discontinuity of S at the Sm-A–N transition. At the nematic side of the N-I transition we found $S=0.50(4)$ (at $P=3.0$) and $S=0.40(4)$ (at $P=2.0$).

In Fig. 8 we show the dependence of the translational order parameter along the director τ on temperature along the different isobars considered in the present work. In the low-temperature crystal phase, this parameter takes on values close to 1 and smoothly decreases with increasing temperature. Typically, the value of τ at the limit of stability of the solid phase is larger the smaller the pressure. A noticeable decrease in the value of τ takes place at the transition to the Sm-A phase (as large as $\Delta\tau\approx0.19$ at $P=3.0$ and $\Delta\tau\approx0.12$ at $P=2.0$). This shows that, as expected, the Cr–Sm-A transition not only involves a two-dimensional in-plane melting but also a lower resolution of the smectic layers when compared to the solid layers. According to our results, the values of τ in the Sm-A side of the Cr–Sm-A transition are seen to decrease almost linearly with increasing pressure. A linear extrapolation to $\tau=0.10$ (typical value of τ found in our finite-size simulations of phases with no translational order) yields the values $P=9.3$ and $P=13.9$ when using the heating and cooling data, respectively. These values give us a rough estimate of the value of the pressure at which the Sm-A is no longer stable.

The (bulk) bond orientational order parameter ψ_6 is displayed in Fig. 9. On heating from the solid phase, ψ_6 decreases with increasing T reaching values between 0.70 and 0.76 at the limit of stability of the crystal phase, the lower values being observed at the higher pressures. On cooling from the fluid phases to the solid, the expected high values of ψ_6 are only attained if a defect-free crystalline structure is grown from the fluid. This process is difficult to achieve (even for the simpler model fluids) and is expected to depend strongly, among other factors, on the particular history of the cooling process. In the present study an almost perfect crystal structure was achieved on cooling at $P=1$ ($\psi_6\approx0.75$). On the other hand, the incomplete crystallization at $P=2$ is

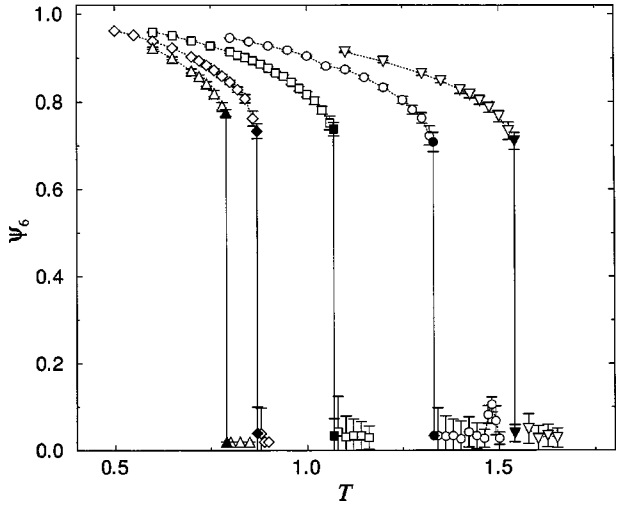

FIG. 9. Variation with temperature T of the (bulk) bond orientational order parameter ψ_6 along the isobars $P=3.0$ (down-triangles), $P=2.0$ (circles), $P=1.0$ (squares), $P=0.4$ (diamonds), and $P=0.2$ (up-triangles). Filled symbols correspond to approximate values at the various transitions.

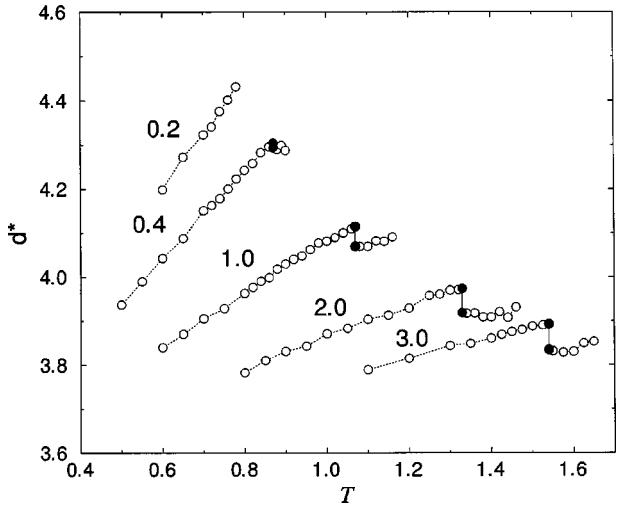

FIG. 10. Variation with temperature T of the layer spacing d^* in the crystal (low temperature) and smectic-A (high temperature) phases obtained in the heating series. Results correspond to different pressures (labeled on the plot). Filled symbols correspond to approximate values at the Cr–Sm-A transition.

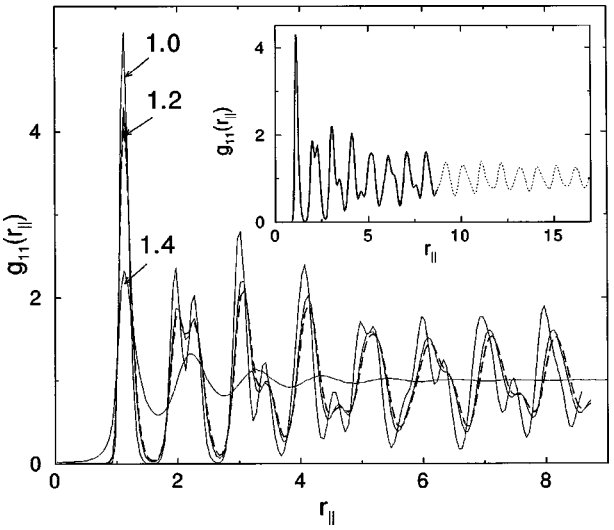

FIG. 11. In-layer positional distribution function $g_{11}(r_\parallel)$ obtained at different temperatures T along the isobar $P=2.0$. Continuous lines are for temperatures $T=1.0$ and 1.2 (Cr phase) and $T=1.4$ (Sm-A phase) along the heating series; discontinuous line is for $T=1.2$ along the cooling run. The inset shows $g_{11}(r_\parallel)$ at $P=2.0$, $T=1.2$ for two system sizes: $N=1640$ molecules (continuous line) and $N=4000$ (dotted line).

manifested by the rather low value of ψ_6 (about 0.45) and a larger volume per particle (see Fig. 2).

The variation of the layer spacing d^* with temperature along the different isobars is presented in Fig. 10. For all pressures investigated here, d^* is observed to increase with increasing temperature along the solid phase. This is the expected mechanical response associated to thermal expansion at constant pressure. At any given temperature, the value of d^* is increasingly higher as the pressure is lowered. Typically, $d^*<\kappa$, and this indicates some degree of interdigitation between adjacent layers (notice, however, that for the smallest pressure considered here, a value $d^*\approx\kappa$ is found at the Cr-I melting transition). In the Sm-A phase, the layer spacing exhibits a weak temperature dependence: although the Sm-A phase extends over a narrow range of temperatures, d^* appears to increase with increasing T. The most striking feature is that the layer spacing clearly decreases at the Cr–Sm-A transition. Recall that the volume of the system increases at the melting transition. In principle, this is due to a nontrivial combination of expansion or compression of the layers and expansion or compression of the system along z. For the present case, the observed compression of the system along z necessarily implies an expansion of the layers at the melting transition. A similar behavior has been reported on theoretical grounds by Velasco and Mederos[14] (although the theoretical analysis was performed there at fixed density) and explained in terms of a nontrivial competition effect between the different contributions to the free energy.

Thus far, the nature of the different phases has been inferred from the behavior of the order parameters. We have found that (a) the low-temperature phase shows crystalline structure; (b) the crystal phase melts into either a Sm-A, an isotropic, or a nematic liquid depending on pressure; and (c) no intermediate Sm-B phase is observed. The above conclusions were further corroborated after analyzing the various structural distribution functions defined in Sec. II B. Here we limit our discussion to phases with either full (crystal) or partial (smectic liquid) translational order. We show in Fig. 11 the in-plane distribution $g_{nn}(r_\perp)$ (for $n=1$) at $P=2.0$ and at several representative temperatures obtained along the heating series. At each thermodynamic condition, all layers displayed the same structure and the corresponding g_{nn} functions were found to be indistinguishable. We recall that the functions $g_{nn}(r_\perp)$ measure positional correlations of the molecules within layer n and so should allow to distinguish between a smectic phase (expected in-plane liquidlike behavior with no long-range structure) and a true crystal phase. At $T=1.0$, this function is highly structured and indicates the existence of positional correlations within the layers. The corresponding function obtained on heating at $T=1.20$ is also presented in the same figure. The peaks are slightly less well resolved and broader as a result of thermal motion; nonetheless, the function still shows considerable crystalline structure and definitely does not correspond to a two-dimensional liquid layer. The same features were observed upon slowly increasing the temperature up to $T=1.32$. Beyond this temperature, the structure changes dramatically, as illustrated in Fig. 11 for $T=1.40$. The structure of the higher temperature phase is that of a system of liquid layers. Whether the structure of this smectic liquid corresponds to a Sm-A or Sm-B phase will become clear shortly.

We recall that BL, simulating large systems, claim that the structure at low temperature (particularly, at $T=1.20$) corresponds to a Sm-B phase. We therefore decided to further investigate the structural properties at $T=1.20$ (and $P=2.0$) considering larger systems. An initial configuration was prepared with four hexagonally ordered layers arranged perpendicular to z with AB packing. The total number of molecules was $N=4000$ and the initial density was $\rho/\rho_{\mathrm{cp}}\approx 0.76$. With this choice of molecular arrangement, the calculation of the in-layer correlation functions can be extended

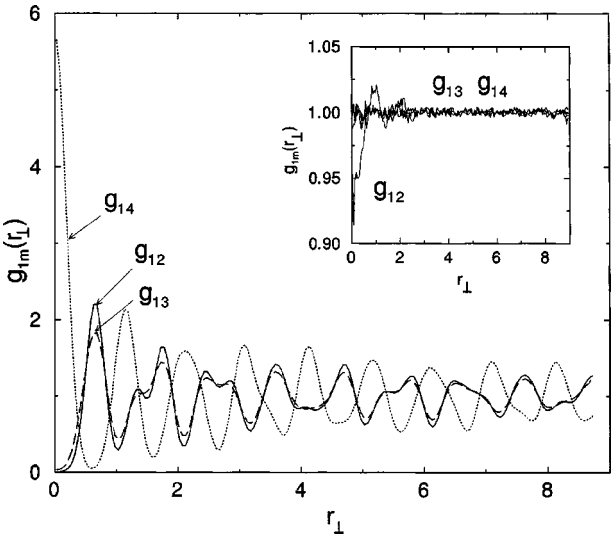

FIG. 12. Interlayer distribution functions g_{1m} between layers 1 and m at pressure $P=2.0$ and temperature $T=1.20$ (crystal phase). Continuous line, $m=2$; long-dashed line, $m=3$; dotted line, $m=4$. The inset shows the same functions in the Sm-A phase ($P=2.0$, $T=1.40$).

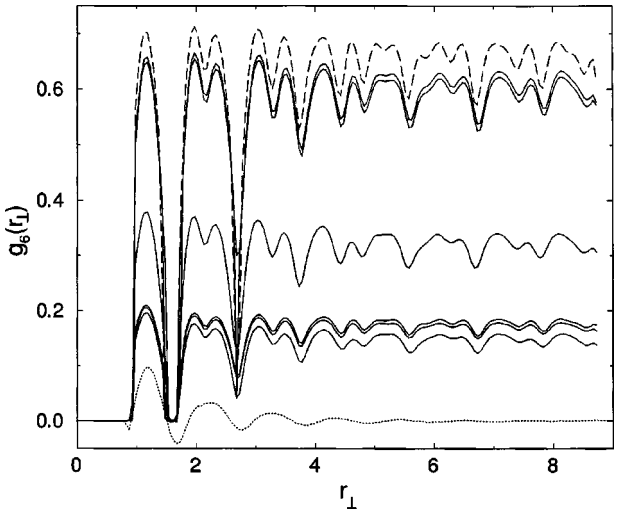

FIG. 13. In-layer bond orientational correlation function for layer m at $P=2.0$ and different temperatures. The long-dashed line corresponds to $m=1$ in the crystal phase at $T=1.20$ along the heating series; the dotted line corresponds to $m=1$ in the Sm-A phase at $T=1.40$ along the heating series; continuous lines are for layers $m=1,2,...,6$ in the (imperfect) crystal at $T=1.20$ along the cooling series.

up to larger distances. After a sufficiently long equilibration, the relevant structural distribution functions were measured. The corresponding in-plane distribution function is shown in Fig. 11 for a given (arbitrary) layer and compared with that obtained under the same thermodynamic conditions for smaller systems ($N=1620$). Both distribution functions exhibit the same structural features and are not consistent with smecticlike behavior. Therefore, our assignment of this phase as a crystal (and not as a Sm-B) appears to have nothing to do with system-size effects. No dependence of the thermodynamic averages on the particular choice of initial structure was seen. This was checked for a number of thermodynamic conditions in the solid and smectic regions.

Further evidence of the crystalline nature of the low-temperature phase were found after analyzing correlations between layers. For a smectic phase (either Sm-A or Sm-B) there should be no long-range positional correlations between the layers.[23] On the other side, a crystal structure should display three-dimensional long-range positional order and so interlayer correlations are expected to be significant. The interlayer distribution functions $g_{1m}(r_\perp)$ (for $m=2$, 3, and 4) obtained at $T=1.20$ are shown in Fig. 12. According to the figure, there are significant positional correlations between layers, and therefore the phase under consideration cannot be considered smecticlike. For comparison, we include in Fig. 12 the corresponding g_{1m} functions obtained in the smectic side of the transition ($T=1.40$).

As argued before, at $P=2.0$ the crystal phase melts into a smecticlike phase at $T=1.33(1)$. The nature of these phases was further probed by computing the in-layer bond orientational correlation functions $g_6^m(r_\perp)$ defined in Eq. (9). Along the heating series, these functions were clearly long range before melting. This is shown in Fig. 13 for one of the (crystal) layers at $T=1.20$ (the same behavior was observed for the rest of the layers). In the smectic side of the transition, however, these functions were short range, the correlations decaying to zero within few oscillations. This behavior is illustrated in Fig. 13 for a representative temperature ($T=1.40$). In agreement with our findings obtained by analyzing the behavior of the order parameters, we conclude that the low-temperature phase is crystalline. In addition, when the crystal melts upon heating into a smectic liquid, the higher temperature phase is Sm-A. Although illustrated here for a single pressure ($P=2.0$), the same structural investigation was carried out at all pressures considered here and the conclusions were the same.

Although no Sm-B phase was found on heating, it still remains to be investigated whether or not a Sm-B phase is developed before crystallization *on cooling* a fluid phase. Again, we consider the case $P=2.0$. Recall that at this pressure, the Sm-A was found to be stable on lowering the temperature up to $T=1.24$. The in-plane distribution function obtained at a lower temperature ($T=1.20$) is shown in Fig. 11 for one of the layers (all other layers exhibited the same features). This function almost coincides with that obtained at the same temperature along the heating series and clearly indicates positional correlations within the layers. This phase exhibits crystalline features and is not a Sm-B phase. The degree of crystallization, however, was found to vary from layer to layer. This is illustrated in Fig. 13, where the in-layer bond orientational correlation function is shown for each individual layer at $T=1.20$. The hexagonal order is significantly high and long range within two of the layers but low (although still long range) within the rest of the layers. As argued before, this is the result of the formation of a distorted lattice structure due to the cooling process. Similar imperfect crystalline structures were found on cooling from a liquid phase at all pressures considered here.

V. CONCLUSIONS

In this paper, we have investigated the phase behavior and structural properties of the GB model by using constant-

pressure Monte Carlo simulation. Although the interactions depend on four parameters, it seems that the gross features of the phase behavior largely depend on the molecular anisotropy κ. For small values of κ, the only stable mesophase is nematic, whereas for larger molecular elongations, the interactions stabilize, in addition, smectic phases. The same qualitative behavior is found for other models (for instance, hard spherocylinders.[20])

An interesting feature of the GB model is that it exhibits pressure-induced mesomorphism.[1,24] For many liquid crystal compounds, the range of stability of the mesophases may increase or decrease under the application of hydrostatic pressure. In addition, mesophases can be induced or even suppressed by the effect of the applied pressure. This is indeed what is observed for the GB model. For the $\kappa=3$ GB model, nematic behavior is only found above a certain value of the pressure.[9,10,12] Similarly, for slightly more anisotropic GB molecules, the Sm-*A* phase enters the phase diagram above a certain pressure.[16] The simulation results reported by Brown *et al.*[16] for GB fluids suggest that the Sm-*A* range does not extend to arbitrarily high pressures. This is consistent with the fact that the effective core of the GB molecules is closely (although not exactly) ellipsoidal and no Sm-*A* phase is expected for hard ellipsoids.[16]

According to a more recent simulation study by Bates and Luckhurst,[17] the $\kappa=4.4$ GB fluid exhibits a further Sm-*B* phase in addition to the Sm-*A* and *N* mesophases. The possibility of the Sm-*B* phase being a crystal, however, was not ruled out.[18] The Sm-*A* range appears to be rather insensitive to pressure over the (narrow) range of pressures ($1\leqslant P\leqslant 3$) considered.[17] We arrive at a similar conclusion for input pressures in that range. An investigation of the model at pressures well outside that range shows, however, that the range of stability of the Sm-*A* does depend on pressure. A nontrivial consequence of this dependence is that the Sm-*A* region is bounded by two end points in a pressure-temperature representation of the phase behavior. This is in agreement with previous investigations of GB fluids[16] where a growth of a stable Sm-*A* ''island'' in the phase diagram was reported for molecular elongations slightly above $\kappa=3$. For the particular case of the $\kappa=4.4$ GB fluid considered here, Sm-*A* behavior appears above $P\approx 0.4$ and disappears at sufficiently high value of the pressure. Assuming a linear behavior of the translational order parameter in the Sm-*A* side of the Cr–Sm-*A* transition, this upper end point is estimated to be somewhere in between $P=9.1$ and 13.9. The absence of Sm-*A* phase at high pressures is seen confirmed from simulations performed at $P=15.0$. At this pressure, the solid melts directly into a nematic liquid characterized by an unusually high degree of orientational order.

At all pressures investigated here, the structure of the low-temperature phase corresponds to a crystal phase. The question of what particular crystalline structure is thermodynamically stable would require free-energy calculations and has not been addressed here. At very high (low) pressures, the solid is seen to melt into a nematic (isotropic) liquid; at intermediate pressures, the crystal melts into a smectic liquid. Analyzing a variety of structural distribution functions, it is concluded that this smectic phase is of the so-called Sm-*A* type. In addition, no intermediate Sm-*B* phase was ever observed. We arrive at the same conclusions after analyzing the behavior of the system along cooling runs. At sufficiently low temperature, the fluid phase (isotropic, nematic, or Sm-*A*, depending on pressure) freezes into a solid structure with lattice defects. On the basis of this and previous investigations, the reported Sm-*B* phase for Gay–Berne models appears to be a molecular solid rather than a smectic liquid phase.

ACKNOWLEDGMENTS

Financial support of the Spanish DGICYT (Dirección General de Investigación Científica y Técnica) under Project No. BFM-2001-1420-C02-02 is acknowledged. Additional support from Universidad de Huelva and Junta de Andalucía is also acknowledged.

[1] S. Chandrasekhar, *Liquid Crystals* (Cambridge University Press, Cambridge, 1977).
[2] P. G. de Gennes and J. Prost, *The Physics of Liquid Crystals*, 2nd ed. (Clarendon, Oxford, 1993).
[3] P. J. Collings and M. Hird, *Introduction to Liquid Crystals* (Taylor and Francis, London, 1997).
[4] See, for example, *Physical Properties of Liquid Crystals*, edited by D. Demus, J. Goodby, G. W. Gray, H.-W. Spiess, and V. Vill (Wiley-VCH, Weinheim, 1999).
[5] S. Singh, Phys. Rep. **324**, 107 (2000).
[6] M. R. Wilson, M. J. Cook, and C. McBride, in *Advances in the Computer Simulations of Liquid Crystals*, edited by P. Pasini and C. Zannoni (Kluwer, Dordrecht, 2000), p. 251.
[7] M. A. Glaser, in *Advances in the Computer Simulations of Liquid Crystals*, edited by P. Pasini and C. Zannoni (Kluwer, Dordrecht, 2000), p. 263.
[8] J. G. Gay and B. J. Berne, J. Chem. Phys. **74**, 3316 (1981).
[9] E. de Miguel, L. F. Rull, M. K. Chalam, K. E. Gubbins, and F. van Swol, Mol. Phys. **72**, 593 (1991).
[10] E. de Miguel, L. F. Rull, M. K. Chalam, and K. E. Gubbins, Mol. Phys. **74**, 405 (1991).
[11] E. de Miguel, Mol. Phys. **100**, 2449 (2002).
[12] E. de Miguel and C. Vega, J. Chem. Phys. **117**, 6313 (2002).
[13] E. Velasco, A. M. Somoza, and L. Mederos, J. Chem. Phys. **102**, 8107 (1995).
[14] E. Velasco and L. Mederos, J. Chem. Phys. **109**, 2361 (1998).
[15] M. P. Allen, J. T. Brown, and M. A. Warren, J. Phys.: Condens. Matter **8**, 9433 (1996).
[16] J. T. Brown, M. P. Allen, E. Martín del Río, and E. de Miguel, Phys. Rev. E **57**, 6685 (1998).
[17] M. A. Bates and G. R. Luckhurst, J. Chem. Phys. **110**, 7087 (1999).
[18] M. A. Bates and G. R. Luckhurst, J. Chem. Phys. **118**, 6605 (2003).
[19] See, for instance, D. Frenkel and B. Smit, *Understanding Molecular Simulation* (Academic, New York, 1996), Chap. 5.
[20] P. Bolhuis and D. Frenkel, J. Chem. Phys. **106**, 666 (1997).
[21] C. Zannoni, in *The Molecular Physics of Liquid Crystals*, edited by G. R. Luckhurst and G. W. Gray (Academic, London, 1979), p. 191.
[22] K. J. Strandburg, in *Bond-orientational Order in Condensed Matter Systems*, edited by K. J. Strandburg (Springer, New York, 1992), Chap 2.
[23] J. W. Goodby, in *Handbook of Liquid Crystals*, edited by D. Demus, J. Goodby, G. W. Gray, H.-W. Spiess, and V. Vill (Wiley-VCH, Weinheim, 1998), Vol. 2A, Chap. 1.
[24] P. Pollmann, in *Physical Properties of Liquid Crystals*, edited by D. Demus, J. Goodby, G. W. Gray, H.-W. Spiess, and V. Vill (Wiley-VCH, Weinheim, 1999), p. 253.